Academic Education Publishing House
*Industry Science and Engineering Vol. 2 No. 10, 2025*

# Analytical Calculation of Catenary Static Geometry Considering Construction Errors

**Jie Yu[1], Jinfa Guan[2,*], Junqing Chen[2], Moran Li[3]**
[1]*Yangtze River Coastal Railway Group Sichuan Co., Ltd., Chengdu, Sichuan, China*
[2]*Southwest Jiaotong University, Chengdu, Sichuan, China*
[3]*China Railways II Engineering Group Limited, Chengdu, Sichuan, China*
**Corresponding Author*

**Abstract: There are many advantages to apply the simple catenary in railway industry, such as simple structure, low investment, convenience repair and good dynamic performance. The simple catenary has been built more and more in the main-lines and the metro. This paper concerns on calculating the static shape of pre-sag contact wire. First, based on the parabola element, the process of calculating the static shape under the influence of the gravitational field and the wind field is given. The equations of the static shape of contact wire and messenger wire in different coordinate systems have been deduced. Finally, by comparing the finite element simulation results, the calculation method has been verified. In addition, it also can calculate the length of the drops and the allowed wind blow.**

**Keywords: Overhead Contact Line; Static Geometry; Construction Deviation; Analytical Calculation**

## 1. Introduction

The static geometric parameters of the contact wire are key parameters characterizing the static performance of the catenary system and exert significant influence on the pantograph-catenary dynamic interaction. Consequently, standards such as Construction Quality Acceptance Standards for High-Speed Railway Electric Traction Power Supply Engineering [1] and Rules for Operation and Maintenance of High-Speed Railway Catenary Systems [2] stipulate strict requirements for construction deviations of contact wire static geometric parameters. Theoretically, precise pre-calculation of catenary static geometry should be performed based on design values of contact wire static geometric parameters before construction, followed by precise prefabrication of droppers and elastic hangers, and precise installation and fixing of the catenary geometry during construction according to pre-calculated positions of droppers and elastic hangers, so as to achieve the design values of contact wire static geometric parameters. However, in practical engineering, construction deviations of contact wire static geometric parameters inevitably arise due to surveying errors, calculation errors, installation errors, environmental condition variations, and other factors. In such cases, the catenary static geometry clearly incorporates construction deviations. It is this catenary static geometry accounting for construction deviations that represents the actual operational condition ultimately delivered to the client and put into service.

Scholars worldwide have conducted certain research on catenary static geometry calculation. References [3-11] discretized the catenary system into several exact cable elements or cable-bar composite elements, cable-beam composite elements, and calculated the static geometry of the catenary system using the nonlinear finite element method to obtain prefabricated lengths of droppers. References [12-15] discretized the catenary into several straight bar elements or parabolic cable elements, catenary cable elements, and calculated the static geometry using classical mechanics methods to determine prefabricated dropper lengths. References [16-18] developed commercial software for catenary dropper prefabrication using computer programming technology based on numerical or analytical calculation methods for catenary static geometry. References [3-11] essentially represent a numerical algorithm for static equilibrium problems of cable-net structures, while references [12-15] constitute an analytical

Academic Education Publishing House

algorithm. Compared with numerical algorithms, analytical algorithms offer advantages such as intuitively reflecting the mathematical and physical relationships among parameters, requiring no iterative integration, and faster computation speed, while demanding less computational expertise from engineers, thus being widely adopted in catenary engineering practice. Currently, research on catenary static geometry calculation focuses on the construction prefabrication stage, with few studies addressing post-construction catenary static geometry calculation. The dropper lengths or force states of the catenary system known to operation and maintenance departments are based on ideal conditions. Therefore, research work on analytical calculation of catenary static geometry accounting for construction deviations is highly necessary.

This study proposes an analytical calculation method for catenary statics using parabolic elements as the fundamental unit and classical mechanics as the computational basis, considering pre-sag of the contact wire, to calculate the static shape of simple catenary suspension under self-weight and under combined effects of lateral wind and self-weight.

## 2. Analytical Calculation Procedure

For actual catenary systems that have been constructed or put into operation, static geometric parameters are measured using catenary detection equipment to analyze the static shape of a pre-sagged simple catenary suspension under self-weight. The procedure begins with a force analysis of the simple catenary suspension, as illustrated in Fig. 1. Based on the pre-sag value (e.g., 0.05% of span length), the approximate static shape of the contact wire with pre-sag is calculated, shown as the dashed line in Fig. 1. Subsequently, the contact wire within each dropper interval is treated as a parabolic element with unequal-height suspension to compute the dropper nodal forces, denoted as $F_1$to $F_5$in Fig. 1. Finally, the moment method is employed to calculate the vertical displacements at each dropper point of the messenger wire under the combined action of dropper forces and self-weight, and the messenger wire within each dropper interval is treated as a parabolic element with unequal-height suspension to determine its static shape. The static calculation flowchart is presented in Fig. 2.

For the analytical calculation of static geometry of catenary systems considering construction deviations, the following assumptions are made:

1)Considering that the catenary system is a simple catenary suspension and the stagger is very small relative to the span, the static geometry of the catenary system is assumed to be in the same plane;

2)Considering that the conductors of a fully compensated catenary suspension are made of similar materials and the tension variation caused by temperature is relatively small, the effect of dropper inclination is neglected;

3)Considering that the nominal span of high-speed railway catenary systems is relatively small, the difference in dropper lengths is minimal, and the self-weight per unit length is low, the self-weight of each dropper is assumed to be identical.

In the absence of measured data for stitch wires and support point construction deviations, the static shape calculation for stitched catenary suspension assumes the following:

1)Considering that the ratio of stagger to span is very small, the static geometry of the catenary suspension in the direction of stagger is neglected;

2)The contact wire has no pre-sag;

3)The height of contact wire dropper suspension points is calculated based on nominal values;

4)Support points, registration points, and stitch wires are at equal elevation;

5)Registration points and support points have the same horizontal coordinate;

6)The tensile deformation of droppers is neglected;

7)The distance from the messenger wire suspension point of the stitch wire to the support point along the track centerline is half the length of the stitch wire;

8)It is assumed that the horizontal tension at the two nodes of a parabolic element is equal in magnitude and opposite in direction;

9)The suspension points of the messenger wire and contact wire have degrees of freedom only along the direction of tension T.

Based on the above assumptions, a mechanical analysis model for the stitched catenary suspension system is established, as shown in Fig. 1. Support point 1 is set as the coordinate origin of the model, and the xoy coordinate system serves as the global coordinate system of the model.

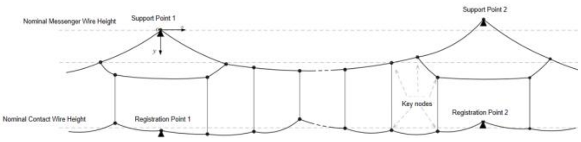


**Figure 1. Schematic Diagram of Key Nodes in Stitched Catenary Suspension System.**

The static shape calculation of a stitched catenary suspension system under self-weight is divided into four steps: first, perform force analysis of the suspension to determine the magnitude and direction of dropper forces and tensions; second, calculate the static shape of the contact wire to obtain dropper nodal forces; third, input these forces into the stitch wires to determine their installation nodal forces; and finally, calculate the static shape of the messenger wire to determine the final dropper lengths. The specific procedure is shown in Fig. 2.

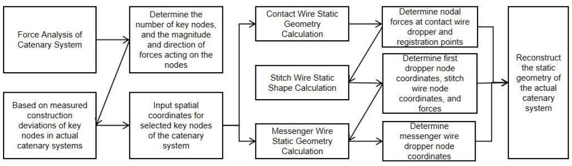


**Figure 2. Analytical Calculation Procedure for Static Geometry of Catenary Systems Considering Construction Errors.**

## 3. Analytical Calculation Method

### 3.1 Contact Wire Static Geometry

The calculation of contact wire static geometry is composed of several parabolic elements with unequal-height suspension, as shown in Fig. 3.

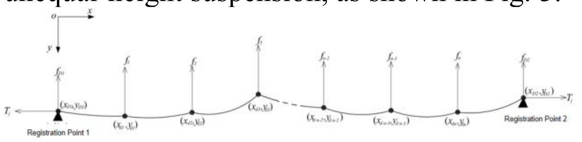


**Figure 3. Static Geometry of Contact Wire Considering Construction Errors.**

Without loss of generality, take a small arc segment between two dropper nodes as an example to calculate its static shape. The actual arc length is approximated by a parabolic element with unequal-height suspension. Since the spatial coordinates of the dropper suspension points are known, the static geometry of the contact wire between any two droppers or between the first dropper and the registration point within a span is given by:

$$y_d = \frac{g_j(x_d - x_{di-1})(x_{di} - x_d)}{2T_j} + \frac{y_{di} - y_{di-1}}{x_{di} - x_{di-1}}(x_d - x_{di-1}) + y_{di-1} \tag{1}$$

$$x_d \in [x_{di-1}, x_{di}], i = 1、\ldots、n、n+1, x_{d0} = x_{D1} = 0, x_{dn+1} = x_{D2} = l$$

Where, $g_j$ is the unit length self-weight of the contact wire (N/m); l is the span length (m).

Thus, the static geometry of the contact wire within each dropper interval is fully determined. Since the shape of a parabolic element is controlled by its two nodes, conversely, the determined static geometry of the contact wire enables calculation of the registration point forces and each dropper nodal force. Furthermore, as each dropper suspends two parabolic elements, the dropper force consists of two components.

In addition to bearing the self-weight of the contact wire, the dropper must also account for its own weight. Since the droppers are relatively lightweight, it is assumed that the self-weight of each dropper is identical, all equal to w.

Based on the force analysis of unequal-height parabolic elements, the internal force of the i-th dropper is:

$$f_i = \frac{g_j(x_{di+1} - x_{di-1})}{2} - \frac{y_{di} - y_{di-1}}{x_{di} - x_{di-1}}T_j + \frac{y_{di+1} - y_{di}}{x_{di+1} - x_{di}}T_j + w \tag{2}$$

$$i = 1, \ldots, n, x_{d0} = x_{D1}, y_{d0} = y_{D1}, x_{dn+1} = x_{D2}, y_{dn+1} = y_{D2}$$

### 3.2 Stitch Wire Static Geometry

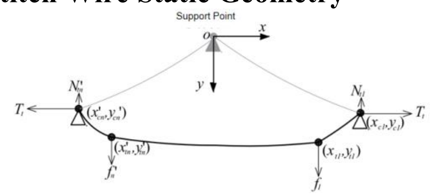


**Figure 4. Stitch Wire Static Geometry.**

The supporting force at suspension point $t_1$ is:

$$N_{t1} = \frac{g_t(x_{c1} - x'_{cn})}{2} + \frac{f'_n(x'_{tn} - x'_{cn}) + f_1(x_{t1} - x'_{cn}) + T_t \cdot (y_{c1} - y'_{cn})}{(x_{c1} - x'_{cn})} \tag{3}$$

$$N'_{tn} = \frac{g_t(x_{c1} - x'_{cn})}{2} + \frac{f'_n(x_{c1} - x'_{tn}) + f_1(x_{c1} - x_{t1}) - T_t \cdot (y_{c1} - y'_{cn})}{(x_{c1} - x'_{cn})} \tag{4}$$

Where, $g_j$ is the unit length self-weight of the stitch wire (N/m).

The stitch wire between suspension point $t_n$ and dropper point n or dropper point 1 is treated as a parabolic element. Since the moment at the node of a parabolic element is zero under static equilibrium, the vertical displacement of the nth dropper node in the adjacent span is:

$$y'_{tn} = \frac{N'_{tn}(x'_{tn} - x'_{cn}) - g_t(x'_{tn} - x'_{cn})^2/2}{T_t} + y'_{cn} \tag{5}$$

$$y_{t1} = \frac{N'_{tn}(x_{t1} - x'_{cn}) - g_t(x_{t1} - x'_{cn})^2/2 - f'_n(x_{t1} - x'_{tn})}{T_t} + y'_{cn} \tag{6}$$

Using the same method described above, the vertical displacement of the nth dropper of the other stitch wire can be readily obtained. At this point, the coordinates of each dropper node of the stitch wire have been determined. The static shape calculation of the stitch wire follows Equation (6). In the xoy coordinate system, the static shape function of the stitch wire is

$$y_t = \frac{g_t(x_t - x'_{cn})(x'_{tn} - x_t)}{2T_t} + \frac{y'_{tn} - y'_{cn}}{x'_{tn} - x'_{cn}}(x_t - x'_{cn}) + y'_{cn}, x_t \in [x'_{cn}, x'_{tn}] \quad (7)$$

$$y_t = \frac{g_t(x_t - x'_{tn})(x_{t1} - x_t)}{2T_t} + \frac{y_{t1} - y'_{tn}}{x_{t1} - x'_{tn}}(x_t - x'_{tn}) + y'_{tn}, x_t \in [x'_{tn}, x_{t1}] \quad (8)$$

$$y_t = \frac{g_t(x_t - x_{t1})(x_{c1} - x_t)}{2T_t} + \frac{y_{c1} - y_{t1}}{x_{c1} - x_{t1}}(x_t - x_{t1}) + y_{t1}, x_t \in [x_{t1}, x_{c1}] \quad (9)$$

As the stitch wire position cannot be measured, the horizontal coordinate is assumed to be the construction prefabrication value.

### 3.3 Messenger Wire Static Geometry

The messenger wire is subjected to its self-weight, intermediate dropper forces, and forces at stitch wire suspension nodes. With a support point as the origin, the xoy coordinate system in Fig. 5 is established. It is assumed that the static shape of the messenger wire consists of several unequal-height suspended parabolic elements, where the horizontal coordinates of each dropper node and stitch wire node are known quantities.

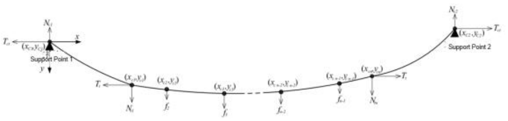


**Figure 5. Messenger Wire Static Geometry.**

First, perform force analysis on the messenger wire. According to the static equilibrium condition of parabolic elements, the horizontal tension at the two nodes is equal in magnitude and opposite in direction, which gives $T_{ct} = T_c - T_t$. Additionally, since the conductor tension from the compensation device to the first stitch wire node is the compensation tension, the messenger wire tension $T_{ct}$ between stitch wires equals the difference between the messenger wire compensation tension $T_c$ and the stitch wire tension $T_t$.

The supporting force at messenger wire support point 2 is:

$$N_{c2} = \frac{g_c(x_{C2} - x_{C1})}{2} + \sum_{i=1}^{n} \frac{f_i(x_{ci} - x_{C1})}{(x_{C2} - x_{C1})} + \frac{T_{ct}(y_{C2} - y_{C1})}{(x_{C2} - x_{C1})}, f_1 = N_{t1}, f_n = N_{tn} \quad (10)$$

$$N_{c1} = \frac{g_c(x_{C2} - x_{C1})}{2} + \sum_{i=1}^{n} \frac{f_i(x_{C2} - x_{ci})}{(x_{C2} - x_{C1})} - \frac{T_{ct}(y_{C2} - y_{C1})}{(x_{C2} - x_{C1})} \quad (11)$$

Where g_c is the unit length self-weight of the messenger wire (N/m).

Therefore, the messenger wire between support point 1 and stitch wire node 1 is treated as a single parabolic element. Since the moment at a parabolic element node is zero under static equilibrium, the vertical displacement of stitch wire node 1 is obtained as:

$$y_{c1} = \frac{N_{c1}(x_{c1} - x_{C1}) - g_c(x_{c1} - x_{C1})^2/2}{T_{ct}} + y_{C1} \quad (12)$$

$$y_{ci} = \frac{N_{c1}(x_{ci} - x_{C1}) - g_c(x_{ci} - x_{C1})^2/2 - \sum_{k=1}^{i-1} f_k(x_{ci} - x_{ck}) + T_{ct}y_{C1} + T_t y_{c1}}{T_c}, i = 2, \ldots, n \quad (13)$$

At this point, the coordinates of each dropper node and stitch wire of the messenger wire have been determined. The static geometry calculation of the messenger wire follows Equation (13). In the xoy coordinate system, the static geometry function of the messenger wire is:

$$y_c = \frac{g_c(x_c - x_{ci-1})(x_{ci} - x_c)}{2T_c} + \frac{y_{ci} - y_{ci-1}}{x_{ci} - x_{ci-1}}(x_c - x_{ci-1}) + y_{ci-1}, x_c \in [x_{ci-1}, x_{ci}] \quad (14)$$
$$i = 1, \ldots, n+1, x_{c0} = x_{C1}, y_{c0} = y_{C1}, x_{cn+1} = x_{C2}, y_{cn+1} = y_{C2}$$

Through the above derivation, the positions of each dropper point and stitch wire node of the messenger wire are obtained. By substituting Equation (12) into Equation (5) and Equation (6), and considering that the stitch wire installation points are at equal elevation, the coordinates of the nth dropper node and the 1st dropper node can be determined. The dropper length is then calculated as:

$$\begin{aligned} c_1 &= D - y_{t1} + y_{C1} \\ c_i &= D - y_{ci} + y_{C1}, i = 2, \ldots, n-1 \\ c_n &= D - y_{tn} + y_{C1} \end{aligned} \quad (15)$$

Where D is the structural height.

### 4. Calculation Example

To verify the accuracy of the proposed calculation method, the catenary system of the Beijing-Shanghai High-Speed Railway is taken as an example. The specific parameters are listed in Table 1.

**Table 1. Design Parameters of Catenary System for Beijing-Shanghai High-Speed Railway.**

| Item | Value | Item | Value |
|---|---|---|---|
| Nominal span l (m) | 50 | Stitch wire length $l_t$ (m) | 18 |
| Messenger wire type | JTMH120 | Stitch wire type | JTMH35 |
| Contact wire type | CTMH150 | Unit length self-weight of stitch wire $g_t$ (N/m) | 0.311*9.8 |
| Unit length self-weight of messenger wire $g_c$ (N/m) | 1.065*9.8 | Stitch wire tension Tt (kN) | 3.5 |

| | | | |
|---|---|---|---|
| Unit length self-weight of contact wire $g_j$(N/m) | 1.350*9.8 | Dropper spacing (m) | 8 |
| Messenger wire tension $T_c$(kN) | 20.0 | Number of droppers | 6 |
| Contact wire tension $T_j$ (kN) | 31.5 | Distance from 1st dropper to registration point (m) | 5 |
| Structural height D (m) | 1.6 | Dropper self-weight (N) | 5 |

A finite element model of the catenary system with identical parameters was established for comparison with the calculation results.

The parameters above were substituted into the aforementioned formulas, and the resulting computational and simulation results are presented in Table 2,Table 3,Table 4 and Table 5. The horizontal coordinates in the tables are very close; to emphasize the vertical coordinates, the horizontal coordinates of the simulation results were rounded.

The comparison shows that the calculated dropper lengths are in very close agreement with the simulation results, with a discrepancy of only approximately 1 mm.

**Table 2. Contact Wire Dropper Node Coordinates and Nodal Forces.**

| Dropper No. | Computational Coordinates (m) | Simulation Coordinates (m) | Computational Nodal Force (N) | Simulation Nodal Force (N) |
|---|---|---|---|---|
| 1 | (5,5.3) | (5,5.3-0.00083) | 86.8950 | 86.46386 |
| 2 | (13,5.3) | (13,5.3-0.00084) | 106.7400 | 106.26526 |
| 3 | (21,5.3) | (21,5.3-0.00088) | 106.7400 | 106.35665 |
| 4 | (29,5.3) | (29,5.3-0.00088) | 106.7400 | 106.35665 |
| 5 | (37,5.3) | (37,5.3-0.00084) | 106.7400 | 106.26526 |
| 6 | (45,5.3) | (45,5.3-0.00083) | 86.89500 | 86.46387 |

**Table 3. Stitch Wire Node Coordinates.**

| Stitch Wire No. | Computational Coordinates (m) | Simulation Coordinates (m) | Dropper No. | Computational Coordinates (m) | Simulation Coordinates (m) |
|---|---|---|---|---|---|
| n | (-9,6.045) | (-9,6.6044) | n | (-5,6.4808) | (-5,6.48127) |
| 1 | (9,6.045) | (9,6.6044) | 1 | (5,6.4808) | (5,6.48127) |

**Table 4. Messenger Wire Dropper Node Coordinates.**

| Dropper No. | Computational Coordinates (m) | Simulation Coordinates (m) | Dropper No. | Computational Coordinates (m) | Simulation Coordinates (m) |
|---|---|---|---|---|---|
| 2 | (13,6.5325) | (13,6.5325) | 4 | (29,6.4564) | (29,6.4563) |
| 3 | (21,6.4564) | (21,6.4563) | 5 | (37,6.5325) | (37,6.5325) |

**Table 5. Dropper Length.**

| Dropper No. | Calculated Length (m) | Simulated Length (m) | Dropper No. | Calculated Length (m) | Simulated Length (m) | Dropper No. | Calculated Length (m) | Simulated Length (m) |
|---|---|---|---|---|---|---|---|---|
| 1 | 1.1808 | 1.1821 | 2 | 1.2325 | 1.2333 | 3 | 1.1564 | 1.1572 |
| 4 | 1.1564 | 1.1572 | 5 | 1.2325 | 1.2333 | 6 | 1.1808 | 1.1821 |

The static geometry of the stitched catenary suspension calculated using this method and that obtained from finite element simulation are shown in Fig. 6, Fig. 7, andFig. 8. As can be seen, except for a certain overall downward displacement of the contact wire simulation curve, the curve shape is in very close agreement with the calculation results (the overall downward displacement is primarily caused by the tensile deformation of the droppers).

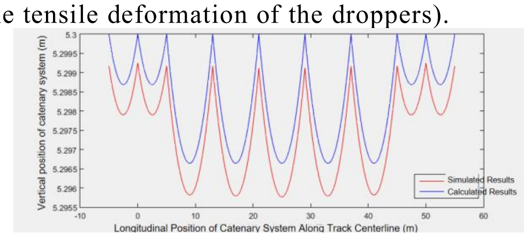


**Figure 6. Static Geometry of Contact Wire Under Self-Weight.**

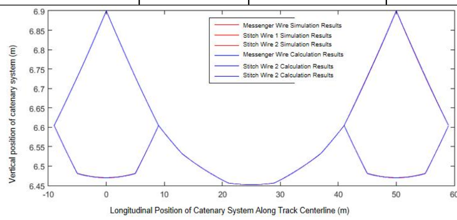


**Figure 7. Static Geometry of Messenger Wire Under Self-Weight.**

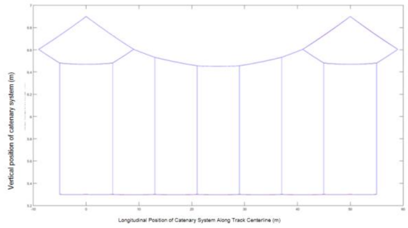

**Figure 8. Static Geometry of Stitched Catenary Suspension Under Self-Weight.**

Construction errors of the catenary system can be obtained by collecting contact wire height data from existing lines. As shown in the lower subfigure of Fig. 9, the contact wire profile from a section of the Beijing-Shanghai High-Speed Railway with relatively poor geometric smoothness exhibits noticeable negative sag at mid-span in the area marked by the red elliptical outline. Applying the algorithm presented in this paper, the geometric shape of the contact wire can be reconstructed, as demonstrated by the comparison between the calculated curve and the measured curve in Fig. 9.

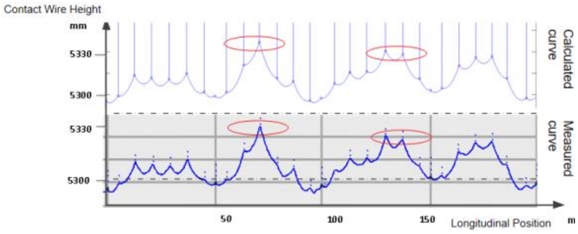


**Figure 9. Comparison of Measured and Reconstructed Contact Wire Geometry for Beijing-Shanghai High-Speed Railway.**

By utilizing measured geometric parameter deviations of the catenary system, the suspension geometry under the combined influence of self-weight and geometric parameter deviations can be analytically calculated, as shown in Fig. 10.

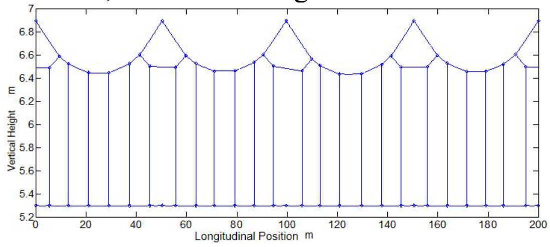


**Figure 10. Static Geometry of Stitched Catenary Suspension Under Self-Weight and Construction Errors.**

## 5. Conclusions

1)This paper first derives the calculation formulas for two types of parabolic elements. Based on these parabolic elements, a calculation procedure for the static shape of simple catenary suspension under self-weight is presented, along with formulas for calculating the static shapes of pre-sagged contact wire and messenger wire in different coordinate systems, and the calculation formula for dropper length.

2)After calculating the static shape of simple catenary suspension under self-weight, the horizontal static shape of the catenary system under lateral wind influence is equivalently represented using parabolic elements. The vertical and lateral static shapes are then synthesized to obtain the three-dimensional static shape of the catenary suspension.

3)Applying this calculation method, the static shapes of the Beijing-Tianjin Intercity Railway catenary under gravity field and under combined gravity field and lateral wind influence are computed. Comparison with finite element simulation results shows that the calculated static shape of the contact wire closely matches the simulation results. The calculated static shape of the messenger wire shows only slightly larger vertical displacement than the simulation results, with the difference being very small (on the order of $10^{-2}$), which meets engineering application requirements. The accuracy of this calculation method is thus verified through comparison with finite element simulation.

4)This research enables dropper prefabrication calculations and wind deflection verification calculations for simple catenary systems, effectively guiding the design and construction of catenary systems.

5)This calculation method is applicable not only to pre-sagged catenary systems but also to catenary systems without pre-sag.

6)It facilitates mastering the actual force state of the catenary system, guiding precise measurement and maintenance of actual catenary systems, and improving the operational quality of catenary systems.

## References

[1]National Railway Administration. TB 10758—2018 Construction Quality Acceptance Standards for High-Speed Railway Electric Traction Power Supply Engineering [S]. Beijing: China Railway Publishing House, 2018.

[2]China Railway Corporation. TG/GD124—2015 Rules for Operation and Maintenance of High-Speed Railway Catenary Systems [S]. Beijing: China Railway Publishing House, 2015.

[3]Yang C J, Zhang W H, Zhang J, et al. Static form-finding analysis of a railway catenary using a dynamic equilibrium method based on flexible multibody system formulation with absolute nodal coordinates and controls [J]. Multibody System Dynamics, 2017, 39(3): 221-247.

[4]Yan Fang, Shibin Gao. Integrated dropper prefabrication for high-speed catenary systems [J]. Journal of Southwest Jiaotong University, 2010, 45(5): 763-767.
[5]Dayong Liu. Research on calculation method of catenary dropper length based on cable net form-finding [D]. Southwest Jiaotong University, 2009.
[6]An Li. Research on static form-finding of high-speed railway catenary systems based on ANSYS [D]. Wuhan University of Technology, 2013.
[7]Yunchang Hou, Zhigang Liu, Yang Song, Ying Wang. 3D static model of electric railway catenary based on cable-bar composite structure [J]. Journal of the China Railway Society, 2014, 36(7): 24-29.
[8]Jie Ruan, Fuwu Yan, Hongmei Li. Establishment of static model for electrified high-speed railway catenary [J]. Journal of the China Railway Society, 2012, 34(8): 20-25.
[9]Fengyuan Li, Jianmin Han, Jianguo Xu, Zhiyong Yang. 3D steady-state model of dropper length for complete anchor section catenary [J]. Railway Standard Design, 2016, 60(7): 134-139.
[10]Hongyu Zhao, Guiming Mei, Haijiang Fan. Accurate calculation of dropper length for flexible catenary [J]. Railway Standard Design, 2011(5): 108-110.
[11]Ruiping Li, Ning Zhou, Guiming Mei, Weihua Zhang. Finite element model of catenary in initial equilibrium state [J]. Journal of Southwest Jiaotong University, 2009, 44(5): 732-737.
[12]Benet J, Cuartero F, Rojo T, et al. Numerical algorithms for the analysis of initial configuration in a railway catenary structure and its code implementation: a software tool CALPE [J]. Mathematical Problems in Engineering, 2015: 1-16.
[13]Jiaxiang Guo, Tianlong Wang. Integrated dropper calculation for high-speed railway catenary based on VBA [J]. Electrified Railway, 2017, 28(3): 53-58.
[14]Jinfa Guan. 3D static shape calculation of pre-sagged catenary [J]. Railway Standard Design, 2013(10): 116-120.
[15]Yang Liu, Nan Wu. Analysis and calculation of catenary anchor joint geometry [J]. Journal of Railway Engineering Society, 2012, 29(5): 49-53.
[16]Cuartero N, Arias E, Cuartero F, et al. CALPE and INDICA. Two tools for calculating the dynamic pantograph/catenary interaction [C]//2012 XXXVIII Conferencia Latinoamericana En Informatica (CLEI). IEEE, 2012: 1-7.
[17]Qianyun Xia . Construction calculation method for copper rod integrated droppers of catenary based on finite element method [J]. China Railway, 2014(6): 59-62.
[18]Cheng Zhang. Development and implementation of dropper prefabrication software for high-speed railway catenary suspension [J]. Railway Computer Application, 2017, 26(11): 5-8.